

2023 Fall Geochemical Thermodynamics

Thermal state and evolving geodynamic regimes of the Meso- to Neoarchean North China Craton

LIANG Xueyin

China University of Geosciences, Beijing
School of Earth Science and Resources
Geology '26

October 25, 2023

Outline

① Basic Information

② Research Method

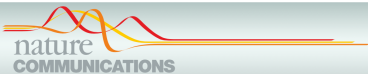
③ Criticism and Implications

④ Reference

1. Basic Information

- ① Journal Information
- ② Why Choose this Article
 - ① Research Gap
 - ② Research Highlight
- ③ Article Information

Journal Information



ARTICLE Check for updates

<https://doi.org/10.1038/s41467-021-24139-z> OPEN

Thermal state and evolving geodynamic regimes of the Meso- to Neoarchean North China Craton

Guozheng Sun¹, Shuwen Liu¹  ^{1✉}, Peter A. Cawood²  ^{2✉}, Ming Tang¹, Jeroen van Hunen³  ³, Lei Gao¹, Yalu Hu¹ & Fangyang Hu^{4,5,6}

Figure 1: Journal Information: Title and Authors

- IF=17.694, H index=248
- Cite By: 35
- JCR: Q1
- Published: 23 June, 2021

Journal Information

Aims & Scope

Nature Communications is an open access, multidisciplinary journal dedicated to publishing high-quality research in all areas of the biological, health, physical, chemical, Earth, social, mathematical, applied, and engineering sciences. Papers published by the journal aim to represent important advances of significance to specialists within each field.

Figure 2: Journal Aims

- Multidisciplinary
- High-quality
- Important Advance of Significance

Background- Previous Study Review

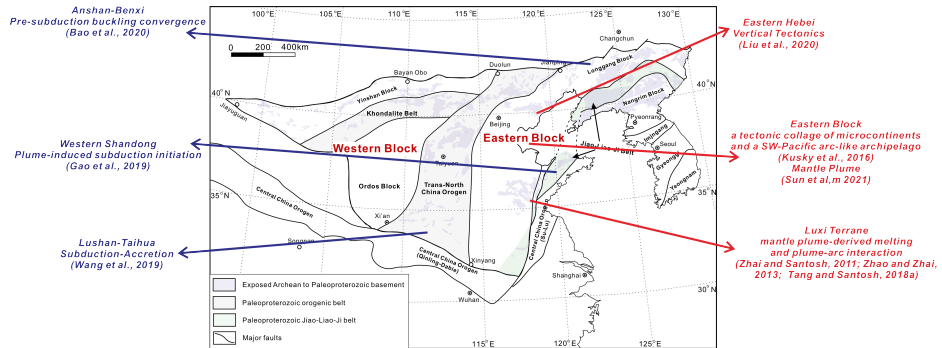


Figure 3: Geological map and the geodynamic Regimes Controversies of the North China Craton (Modify from Zhao et al., 2013)

Background- Basic Concepts

- 地幔潜能温度 (Mantle Potential Temperature): 地幔在未减压和未熔融的前提下上升到地表过程的假设温度 (Putirka, 2005)
- 地温梯度 (Geothermal Gradient): 指地壳的地温随深度增加而升高的数值
- 热流值 (Heat Flow): 指单位时间内通过单位面积的热流量
- 不同大地构造背景下具有不同的热流值和地温梯度

Background- Mantle Potential Temperature

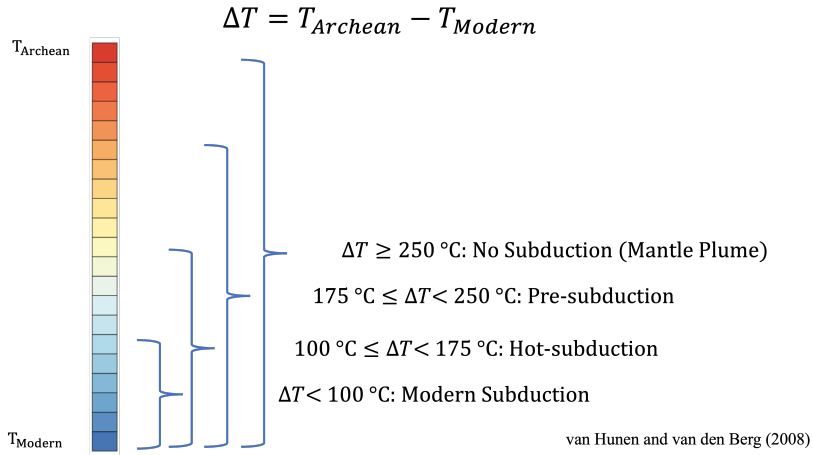


Figure 4: Mantle Potential Temperature and Geodynamic regimes

Why Choose this Article

- Research Gap:
 - ① Dynamic Mechanism Controversies: Mantle Plume or Plates Subduction (**Conditions? and Initial Time?**)
(Bédard, 2006; Dhuime et al., 2012; Johnson et al., 2013; Tang et al., 2016; Cawood et al., 2018; Cawood and Hawkesworth, 2019; Brown et al., 2020)
 - ② Few researches focus on calculating **Crustal thickness, Moho temperature, and heat flow**
(Davies, 2006; Turcotte and Schubert, 2014; Capitanio et al., 2019b; Chowdhury et al., 2020)
 - ③ Apparent geothermal gradient \neq Moho geothermal gradient
 - ④ Thermal mechanic modeling results lack of geological evidence
 - ⑤ Traditional geophysical methods are ineffective for the study of the early Earth's thermal state

Why Choose this Article

- Research Highlight:
 - ① Limited the thermal state, thickness and rigidity of the continental crust
 - ② Thermal structure of the Meso- to Neoarchean continental lithosphere has been reconstructed by mathematical modelling
 - ③ Provide important new insight in Archean geodynamic regimes

Article Information

- Research Focus: Geodynamic Regimes of the Early Earth (Precambrian)
- Research Object: multiple periods of Archean tonalite- trondhjemite- granodiorite (TTG) gneisses
- Research Aims: Explore the petrogenesis of Meso- to Neoarchean granitoids and their inferred lithospheric thermal states and crust-mantle dynamics

2. Research Method

① Thermodynamic and trace element modelling

- ① TTG Selection
- ② Selection of Mafic Source Rocks of the TTG Magmatism
- ③ Define protolith and water content
- ④ Thermodynamic Modelling of Primary Magma (By Software PerpleX)
- ⑤ Batch Partial Melting Modeling

② Thermal Structure Calculating

- ① Geothermal Model

Estimation of the thermal state for NCC

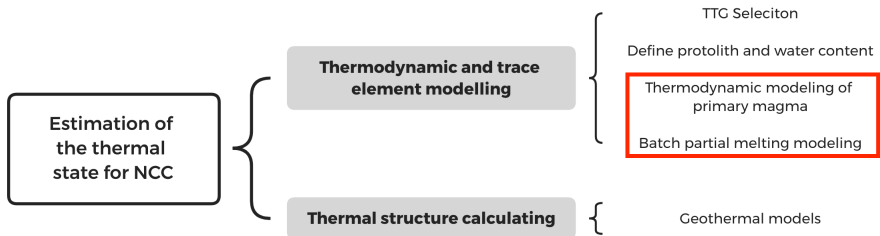


Figure 5: Process of Methods

Thermodynamic- TTG Selection

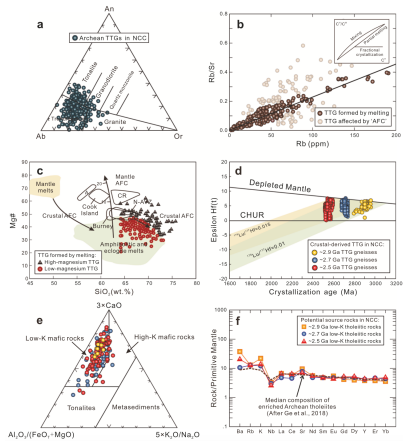


Figure 6: Geochemical Characteristics
(Sun et al., 2021)

Derived from the base of the crust (Mafic Source)

- Exclude samples with heterogeneous whole-rock Nd and zircon Hf isotopic compositions
- Derived from partial melting
- Lower Mg# significantly (Mean < 38)
- Lower LOI and slightly Ce anomalies

Thermodynamic- Define protolith and water content

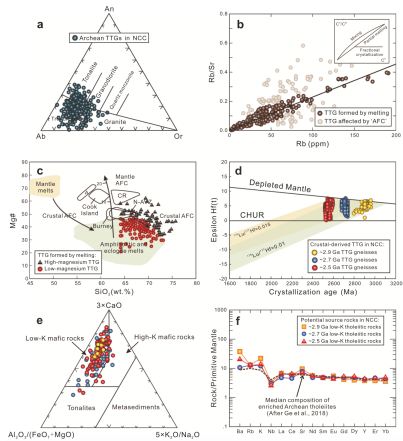


Figure 7: Geochemical Characteristics
(Sun et al., 2021)

- Ideal Source Rocks: **Enriched Archean tholeiites** (Martin et al., 2014)
- Low K (Figure 6e)
- $X(H_2O)$ defined by LOI (Palin et al., 2016a)
- Nearly flat REE pattern
- Multiple episodes (Figure 6f)

Thermodynamic- Thermodynamic modeling of primary magma

- Software: Perple_X (version 6.9.0)
- System: NCKFMASHTO
- Object: Average composition of ~ 2.9 , ~ 2.7 , and ~ 2.5 low-K tholeiitic rocks
- Discrete P-T points: every $10\text{ }^{\circ}\text{C}$ and 0.1 GPa from 750 to $950\text{ }^{\circ}\text{C}$ and 0.6 to 2.0 GPa,
- Water content: 1.6, 1.8, 2.0 wt.%

Thermodynamic- Thermodynamic modeling of primary magma

Stable phases at:														
	T(K)	=	1133.00											
	P(bar)	=	8000.00											
Phase Compositions (molar proportions):														
	wt %	vol %	mol %	mol	H2O	MgO	Al2O3	SiO2	K2O	CaO	TiO2	FeO	Fe2O3	Na2O
cAmph(G)	46.39	43.62	15.08	0.519E-01	0.87916	2.26537	1.40090	6.08359	0.01668	1.53467	0.24168	1.82764	0.10817	0.29875
Augite(G)	17.47	15.51	22.00	0.756E-01	0.00000	0.68325	0.05332	1.93307	0.00000	0.84690	0.00000	0.44421	0.02329	0.00968
melt(G)	18.19	23.83	41.64	0.143	0.45695	0.08899	0.17525	1.42751	0.02397	0.09123	0.00000	0.04381	0.00000	0.05715
Gt(W)	8.46	6.48	5.21	0.179E-01	0.00000	0.67814	0.95295	3.00000	0.00000	0.64748	0.00000	1.67439	0.04705	0.00000
Fsp(C1)	7.73	8.62	8.17	0.281E-01	0.00000	0.00000	0.85580	2.28839	0.00196	0.71161	0.00000	0.00000	0.00000	0.14223
Ilm(WPH)	0.19	0.13	0.38	0.129E-02	0.00000	0.09232	0.00000	0.00000	0.00000	0.00000	0.96143	0.86912	0.03857	0.00000
q	1.56	1.83	7.53	0.259E-01	0.00000	0.00000	0.00000	1.00000	0.00000	0.00000	0.00000	0.00000	0.00000	0.00000

Figure 8: Thermodynamic Modeling Results

- To get melt composition and degree of partial melting.

Thermodynamic- Batch partial melting modeling

- To calculate the trace element composition of the TTG melts.

Batch partial melting equation (Shaw, 1970):

$$\frac{C_{melt}}{C_{Source}} = \frac{1}{D + F \times (1 - D)} \quad (1)$$

C_{Source} : The average composition of the ~2.9, ~2.7 and ~2.5 Ga low-K tholeiitic rocks

C_{Melt} : median composition of TTG melts

D : partition coefficient of minerals

(from: <https://earthref.org/GERM/KDD/>)

Thermodynamic- Result

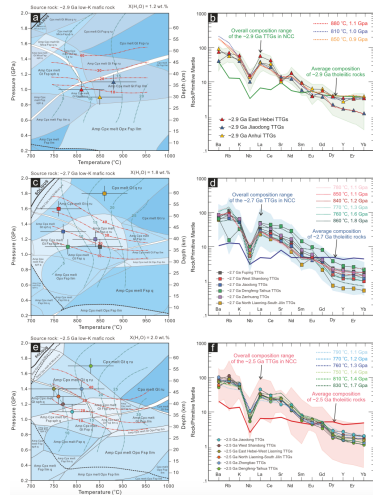


Figure 9: Modeling (Sun et al., 2021)

- Select sample closing to actual TTG
- Pressure: a minimum estimate of crustal thickness
($1 \text{ Gpa} \approx 33 \text{ km}$)
- Temperature: the lower limit of Moho temperature

Geothermal Models

Temperature and Heat Flow (Chapman, 1986)

$$T_B = T_T + \frac{q_t}{k} \Delta z - \frac{A \Delta Z^2}{2k} \quad (2)$$

$$q_B = q_t - A \Delta Z \quad (3)$$

where ΔZ is crustal thickness, A, k is layer properties, T_B is Moho surface temperature, and define Land Surface Temperature $T_T = 0$

And Land Surface heat flow q_t is?

The *Volumetric Heat Production* in the crust (Tang et al., 2020)

$$A_j = \sum_j F_j \rho \sum_i H_i C_j^i e^{-\lambda_i t} \quad (4)$$

Geothermal Models

Fourier's law

$$q_B = -k \frac{\Delta T}{\Delta x} \quad (5)$$

In this case, the $\frac{\Delta T}{\Delta x}$ represent **the geothermal gradient slope of Moho Surface.**

Result

Table 1 Key values of calculated Meso- to Neoarchean thermal state of the Eastern Block, North China Craton.

Era and location	Melting temperature (°C)	Melting pressure (GPa)	Crustal thickness (km)	q_B (mW m ⁻²)	Moho geothermal gradient (°C/km)
-2.9 Ga					
Jiaodong	880 ± 50	1.1 ± 0.1	33-39	46-65	18-25
Anhui	850 ± 50	0.9 ± 0.1	27-33	55-80	21-31
East Hebei	810 ± 50	1.0 ± 0.1	30-36	46-67	18-26
-2.7 Ga					
North Liaoning-South Jilin	860 ± 50	1.8 ± 0.1	56-62	18-28	7-11
West Shandong	760 ± 50	1.6 ± 0.1	50-56	19-30	7-11
Jiaodong	770 ± 50	1.3 ± 0.1	40-46	29-43	11-17
Fuping	850 ± 50	1.1 ± 0.1	33-40	42-63	16-24
Zanhuan	840 ± 50	1.2 ± 0.1	37-43	37-53	14-20
Dengfeng-Taihua	780 ± 50	1.1 ± 0.1	33-40	37-57	14-22
-2.5 Ga					
North Liaoning-South Jilin	760 ± 50	1.3 ± 0.1	40-46	29-43	11-16
West Shandong	770 ± 50	1.2 ± 0.1	37-43	33-48	13-19
Jiaodong	790 ± 50	1.1 ± 0.1	33-40	38-50	15-22
East Hebei-West Liaoning	750 ± 50	1.4 ± 0.1	43-50	24-38	9-14
Dengfeng-Taihua	830 ± 50	1.7 ± 0.1	53-59	20-30	8-12
Zhongtiao	810 ± 50	1.4 ± 0.1	43-50	27-41	10-16

Figure 10: Results of Key values (Sun et al., 2021)

Result

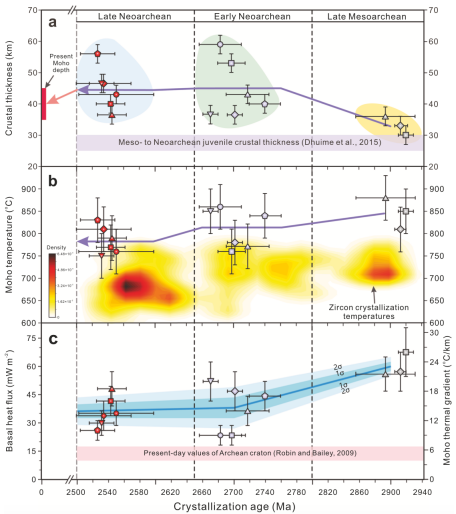


Figure 11: Changes of key values (Sun et al., 2021)

Result

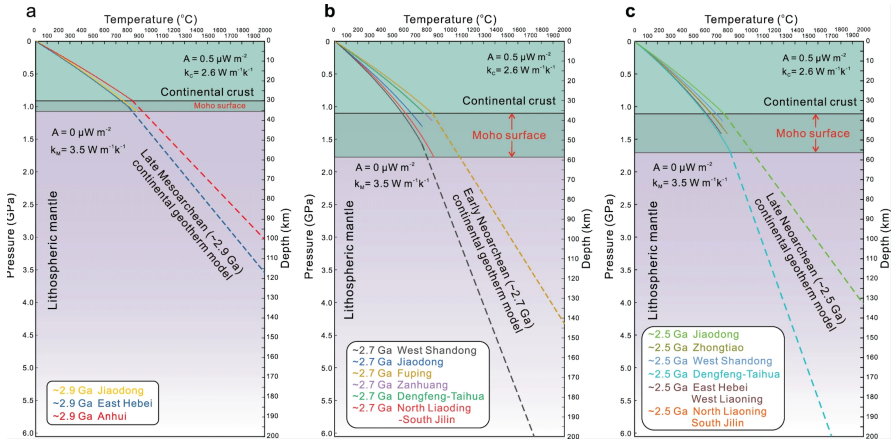


Figure 12: Generic model (Sun et al., 2021)

Result

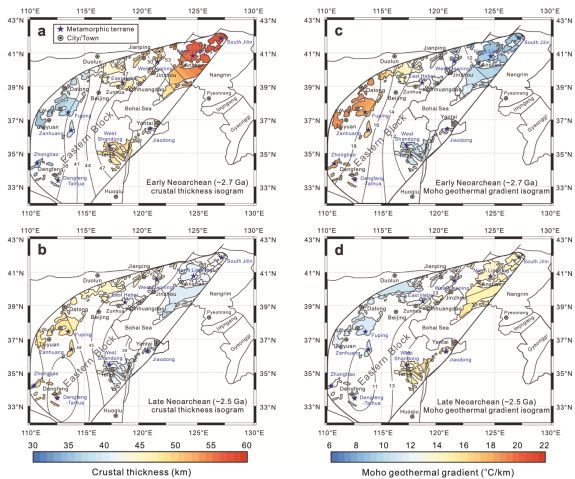


Figure 13: Contour color plots of crustal thickness and Moho geothermal gradient (Sun et al., 2021)

Research Conclusion

The geodynamic evolution of the Meso-Neoarchaean in the Eastern Block of North China Craton is divided into three stages:

- ① Late Mesoarchean (2.9-2.8 Ga):

Higher mantle potential temperature and **thinner** lithospheric thickness \implies **Mantle Plume**

- ② Early Neoarchean (2.7 Ga):

Crustal thickness began to **increase** rapidly \implies **Plate Tectonics**

- ③ Late Neoarchean (2.7-2.5 Ga):

Marginal lateral accretion \implies **Hot subduction**

3. Criticism and Implications

- ① Criticism
- ② Implications

Criticism

- One-dimensional heat conduction model: the dimensions of the terms on the left and right sides of the equation **are not equal**.
- Indicates the absence of a significant physical quantity in the equation.

Implications

- Provide methods to **estimate the thickness of the Earth's crust** and its **thermal state** during various geological epochs.
- Analyze when the structural regimes of the major cratons **transition from vertical tectonics to horizontal tectonics**.
- Provide unique insights into **the timing of the initiation of plate tectonics** on a global scale (initiated globally **at the same time or sequentially** in various major cratons).

Reference

- [1] Bao, H., Liu, S.W., Wang, M.J., Teng, G.X., Sun, G.Z., 2020. Mesoarchean geodynamic regime evidenced from diverse granitoid rocks in the Anshan-Benxi area of the North China Craton. *Lithos* 366, 105574.
- [2] Bédard, J. H., 2006. A catalytic delamination-driven model for coupled genesis of Archaean crust and sub-continental lithospheric mantle. *Geochimica et Cosmochimica Acta* 70, 1188–1214.
- [3] Brown, M., Johnson, T., Gardiner, N.J., 2020. Plate Tectonics and the Archean Earth. *Annual Review of Earth and Planetary Sciences* 48, 291–320.
- [4] Capitanio, F.A., Nebel, O., Cawood, P.A., Weinberg, R.F., Clos, F., 2019b. Lithosphere differentiation in the early Earth controls Archean tectonics. *Earth and Planetary Science Letters* 525, 1–12.
- [5] Cawood, P.A., Hawkesworth, C.J., 2019. Continental crustal volume, thickness and area, and their geodynamic implications. *Gondwana Research* 66, 116–125.

Reference

- [6] Cawood, P.A., Hawkesworth, C.J., Pisarevsky, S.A., Dhuime. B., Capitanio. F.A., Nebel, O., 2018. Geological archive of the onset of plate tectonics. *Philosophical Transactions of the Royal Society a-Mathematical Physical and Engineering Sciences* 376(2132), 1–30.
- [7] Chapman, D.S., 1986. Thermal gradients in the continental crust. *Geological Society of London, Special Publications* 24, 63–70.
- [8] Chowdhury, P., Chakraborty, S., Gerya, T.V., Cawood, P.A., Capitanio, F.A., 2020. Peel-back controlled lithospheric convergence explains the secular transitions in Archean metamorphism and magmatism. *Earth and Planetary Science Letters* 538, 116224.
- [9] Davies, G.F., 2006. Gravitational depletion of the early Earth's upper mantle and the viability of early plate tectonics. *Earth and Planetary Science Letters* 243, 376–382.
- [10] Dhuime, B., Hawkesworth, C.J., Cawood, P.A., Storey, C., 2012. A change in the geodynamics of continental growth 3 billion years ago. *Science*, 335(6074): 1334-1336.

Reference

- [11] Gao, L., Liu, S.W., Zhang, B., Sun, G.Z., Hu, Y.L., Guo, R.R., 2019. A ca.2.8 Ga plume-induced intraoceanic arc system in the eastern North China craton. *Tectonics*, 38(5): 1694-1717.
- [12] Johnson, T.E., Brown, M., Kaus, B.J.P., VanTongeren, J.A., 2013. Delamination and recycling of Archaean crust caused by gravitational instabilities. *Nature Geoscience* 7, 47–52.
- [13] Liu, T., Wei, C.J., 2020. Metamorphic P T paths and Zircon U-Pb ages of Archean ultra-high temperature paragneisses from the Qian' an gneiss dome, East Hebei terrane, North China Craton. *Journal of Metamorphic Geology*, 38: 329-356.
- [14] Martin, H., Moyen, J.F., Guitreau, M., Blichert-Toft, J., Le Pennec, J.L., 2014. Why Archaean TTG cannot be generated by MORB melting in subduction zones. *Lithos*, 198, 1–13.
- [15] Palin, R.M., White, R.W., Green, E.C.R., 2016a. Partial melting of metabasic rocks and the generation of tonalitic–trondhjemite–granodioritic (TTG) crust in the Archaean: Constraints from phase equilibrium modelling. *Precambrian Research* 287, 73–90.

Reference

- [16] Shaw, D.M., 1970. Trace element fractionation during anatexis. *Geochimica et Cosmochimica Acta* 34, 237–243 (1970).
- [17] Tang, M., Chen, K., Rudnick, R.L., 2016. Archean upper crust transition from mafic to felsic marks the onset of plate tectonics. *Science* 351, 372–375.
- [18] Tang, M., Lee, C.T., Rudnick, R.L., Condie, K.C., 2020. Rapid mantle convection drove massive crustal thickening in the late Archean. *Geochimica et Cosmochimica Acta* 278, 6–15.
- [19] Tolstikhin, I., Kramers, J., 2008. *The Evolution of Matter: From the Big Bang to the Present Day*. Cambridge University Press.
- [20] Wang, X., Huang, X.L., Yang, F., 2019. Revisiting the Lushan-Taihua Complex: New perspectives on the Late Mesoarchean-Early Neoarchean crustal evolution of the southern North China Craton. *Precambrian Research*, 325: 132-149.
- [21] Z Zhao, G.C., Zhai, M.G., 2013. Lithotectonic elements of Precambrian basement in the North China Craton: Review and tectonic implications. *Gondwana Research*, 23: 1207-1240.

Thanks for your listening!

November 13, 2025